Chemical Engineering Journal 513 (2025) 162921

Contents lists available at ScienceDirect

Chemical Engineering Journal

journal homepage: www.elsevier.com/locate/cej

Polyhalogenated heterocycle additive induced in-situ 3D gelatinous polymerization with polysulfides for shuttle effect inhibited lithium-sulfur batteries

Xingkai Ma [a], Xinmei Song [a], Yaoda Wang [a], Junchuan Liang [a], Tianyu Shen [a], Zuoao Wu [a], Lina Qin [a], Huan Li [a], Tianchen Yu [a], Huaizhu Wang [a], Zuoxiu Tie [a,*], Yichao Yan [a,*], Lin Sun [a,b,*], Zhong Jin [a,*]

[a] State Key Laboratory of Coordination Chemistry, MOE Key Laboratory of Mesoscopic Chemistry, MOE Key Laboratory of High Performance Polymer Materials and Technology, Jiangsu Key Laboratory of Advanced Organic Materials, Suzhou Key Laboratory of Green Intelligent Manufacturing of New Energy Materials and Devices, Tianchang New Materials and Energy Technology Research Center, Institute of Green Chemistry and Engineering, School of Chemistry and Chemical Engineering, Nanjing University, Nanjing, Jiangsu 210023, PR China

[b] School of Chemistry and Chemical Engineering, Yancheng Institute of Technology, Yancheng 224051, PR China

ARTICLE INFO

Keywords:
Lithium-sulfur batteries
In-situ polymerization
Shuttle effect inhibited
Organosulfur cathodes

ABSTRACT

Lithium-sulfur (Li-S) batteries hold immense promise for achieving high energy density and cost-effectiveness; however, they are plagued by rapid capacity fade and decreased efficiency due to the polysulfide shuttle effect. Herein, we report the introduction of a small molecule additive, tetrachloropyrimidine (TCPy), into ether-based electrolytes to trigger in-situ 3D gelatinous polymerization with polysulfides. The chlorine atoms in TCPy initiated nucleophilic substitution reactions with formerly soluble polysulfides, leading to the formation of an insoluble 3D-crosslinked and gelified organosulfur polymer network that effectively inhibits the polysulfide shuttle effect and preserves high active sulfur content. The abundant nitrogen sites in TCPy exhibit high conductivity and strong chemical adsorption towards polysulfides, thus further enhancing the kinetics of sulfur redox reactions. Consequently, the incorporation of TCPy additive in the electrolyte significantly mitigates the capacity degradation caused by polysulfide shuttling, and dramatically improves the rate capability and cycling stability of Li-S batteries, without reducing the active sulfur content in the cathode. This study underscores the enormous potential of additive-induced in-situ gelatinization strategy for effectively binding, blocking and sequestering polychalcogenides, thereby elevating the overall performance of rechargeable alkali metal–chalcogen batteries.

1. Introduction

Lithium-sulfur (Li-S) batteries have emerged as a promising contender for future energy storage systems, attributed to their remarkable theoretical energy density and eco-friendly nature.[1–9] However, their practical applications still face several formidable challenges, including the inherent poor conductivity of sulfur cathode, the detrimental shuttle effect of polysulfides, and the uncontrolled dendrite growth of the lithium anode. These issues collectively result in progressive capacity fading and overall performance degradation over time.[10–16] Particularly, the shuttle effect poses a significant obstacle, as it leads to the loss of active sulfur species and a subsequent decline in battery capacity.[17–21] Researchers have dedicated considerable efforts to developing innovative strategies aimed at immobilizing and stabilizing polysulfides.[22–30] One promising approach involves the synthesis of organosulfur cathode materials, where active sulfur species are covalently bonded to organic molecular frameworks.[31–37] The covalent anchoring can alleviate the formation of polysulfides and retards their migration within the battery. However, there exists a tradeoff between the integration of organic frameworks and the decrease in active sulfur content within these organosulfur cathodes. It is imperative to overcome this obstacle, meanwhile preserving a high active sulfur content that is crucial for sustaining the high energy density of Li-S batteries.

* Corresponding authors.
E-mail addresses: zxtie@nju.edu.cn (Z. Tie), ychyan@nju.edu.cn (Y. Yan), chem_sun@ycit.edu.cn (L. Sun), zhongjin@nju.edu.cn (Z. Jin).

https://doi.org/10.1016/j.cej.2025.162921
Received 24 March 2025; Received in revised form 10 April 2025; Accepted 20 April 2025
Available online 21 April 2025

In pursuit of this objective, here we propose a promising strategy that introduces small-molecule electrolyte additives to initiate co-polymerization with polysulfides, leading to the in-situ formation of organosulfur polymers. Specifically, we utilize a small organic molecule, tetrachloropyrimidine (TCPy), characterized by its chlorine content and high solubility in ether-based electrolytes, as an electrolyte additive to achieve covalent anchoring of polysulfides and inhibit the shuttle effect. The formally soluble polysulfides undergo nucleophilic substitution reactions with the Cl sites in TCPy, initiating a 3D cross-linked gelatinous polymerization process to produces an organosulfur polymer insoluble in the electrolyte. Furthermore, the abundant N sites in TCPy exhibit strong chemical adsorption capabilities towards polysulfides, furthering improving the kinetics of sulfur redox reactions. Consequently, the TCPy-modified electrolyte significantly alleviates the capacity degradation associated with the shuttle effect, thereby substantially improving the rate performance and cycle stability of Li-S batteries without compromising the active sulfur content in the cathode. The Li-S batteries modified with TCPy additive demonstrate a high specific capacity of 700.7 mAh g^{-1} after 200 cycles at 2.0 C and an improved rate performance of 660.0 mAh g^{-1} at 4.0 C. Furthermore, a notable decrease in polysulfide dissolution and capacity degradation has been observed, confirming the enhanced cycling stability achieved through this strategy. This study underscores the immense potential of functional electrolyte additives in enabling in-situ covalent anchoring and gel polymerization of polychalcogenides, thereby simultaneously achieving high energy density and prolonged cycling stability in rechargeable alkali metal–chalcogen batteries.

2. Result and discussion

The introduction of TCPy additive in electrolyte can initiate the in-situ crosslinked polymerization of soluble polysulfide anions with TCPy molecules during the discharge processes of Li-S batteries. As depicted in Fig. 1a, when long-chain polysulfides with high solubility start to form (corresponding to when the battery is discharged to around 2.20 V), the added TCPy molecules undergo nucleophilic substitution reactions with these polysulfides, thus in-situ generating insoluble polysulfide-tetra-substituted pyrimidine (PSTPy) on the surface of the cathode. In contrast, Fig. S1 illustrated the discharge process diagram of traditional Li-S batteries without TCPy additive, wherein exhibited a severe shuttle effect caused by the dissolution of long-chain polysulfides in the electrolyte. The optimized structure and electrostatic potentials of

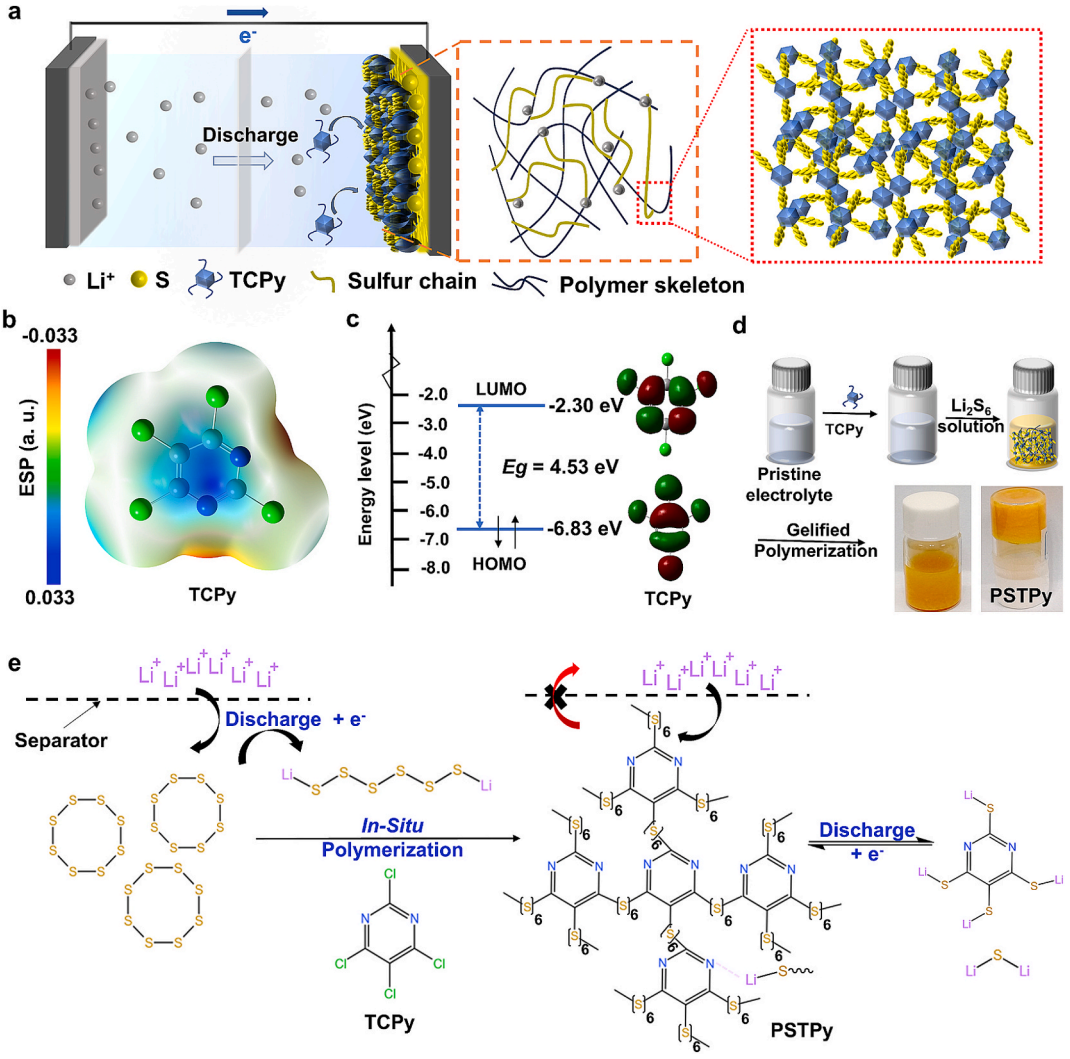

Fig. 1. (a) Schematic diagram of the 3D crosslinked gelling polymerization reaction induced by TCPy additive in ether-based electrolyte during the discharge process of Li-S batteries. (b) Optimized structure and electrostatic potentials of TCPy. (c) Molecular orbitals and energy gaps of TCPy. (d) The 3D gelatinous polymerization phenomenon of polysulfides by adding Li_2S_6 solution (0.4 M Li_2S_6 in a 1:1 (v/v) dimethoxymethane (DME)/1,3-dioxolane (DOL) mixture) into the TCPy-modified electrolyte (1.0 M LiTFSI dissolved in a 1:1 (v/v) DME/DOL mixture with 1.0 wt% $LiNO_3$ and 50 mM TCPy additive). (e) Modified working mechanism of sulfur cathode in TCPy-modified electrolyte.

TCPy molecule are shown in Fig. 1b. The greater negativity of the electrostatic potential at the N-atom site, indicating its stronger electron-withdrawing capability, thus resulting in an enhanced ability of TCPy molecule to adsorb polysulfides. Conversely, the carbon atoms show the most positive electrostatic potential, suggesting susceptibility to nucleophilic substitution. This allows the chlorine site to be replaced by polysulfide ions, leading to the formation of 3D-crosslinked PSTPy gelatin. The energy levels of the lowest unoccupied molecular orbital (LUMO) and the highest occupied molecular orbital (HOMO) of TCPy molecule are also calculated (Fig. 1c). Compared to the LUMO of DME or DOL solvent molecules at the same computational level (Fig. S2), the elevated LUMO value of TCPy molecule suggested its resistance to reduction reactions, thus affirming its potential to uphold structural stability when employed as an electrolyte additive.

To demonstrate that the TCPy molecule can react with polysulfides generated during the discharge process of Li-S batteries, 1.5 mL of 0.4 M Li_2S_6 solution in dimethoxymethane (DME)/1,3-dioxolane (DOL) 1:1 (v/v) mixture was prepared and added into the electrolyte with and without TCPy additive (Fig. 1d and Fig. S3). It could be seen that the TCPy-modified electrolyte was turned into a brown transparent gelatin with poor fluidity after the addition of Li_2S_6 solution. Conversely, the color of pristine electrolyte after mixing with Li_2S_6 solution remained unchanged and formed no precipitate. These results further verified that the TCPy molecule could react with the Li_2S_6 to form 3D-crosslinked PSTPy gelatin.

The in-situ gelatinous polymerization mechanism of TCPy and polysulfides (such as Li_2S_6) was illustrated in Fig. 1e. The TCPy molecule was rich in multiple chlorine atoms and provided abundant nucleophilic substitution sites for polysulfides.[38] Furthermore, the N-atom sites on TCPy molecule had a certain adsorption capacity for polysulfides.[39] These factors facilitate the incorporation of polysulfides with TCPy, resulting in the formation of an insoluble network-crosslinked PSTPy gelatin. Consequently, the shuttle effect is significantly mitigated, leading to highly improved cycling lifespan of Li-S batteries.

The network-crosslinked structure of PSTPy gelatin were systematically identified by attenuated total reflection-Fourier transform infrared (ATR-FTIR) spectroscopy, Raman spectroscopy and X-ray photoelectron spectroscopy (XPS). As depicted in Fig. 2a, the ATR-FTIR spectra of PSTPy showed a prominent peak at approximately 1190 cm^{-1}, which is ascribed to the formation of C—S bonds. Notably, the intensity of the C—Cl peak at around 700 cm^{-1} notably decreased compared to the TCPy precursor. This suggests that a considerable portion of Cl^- ions in TCPy

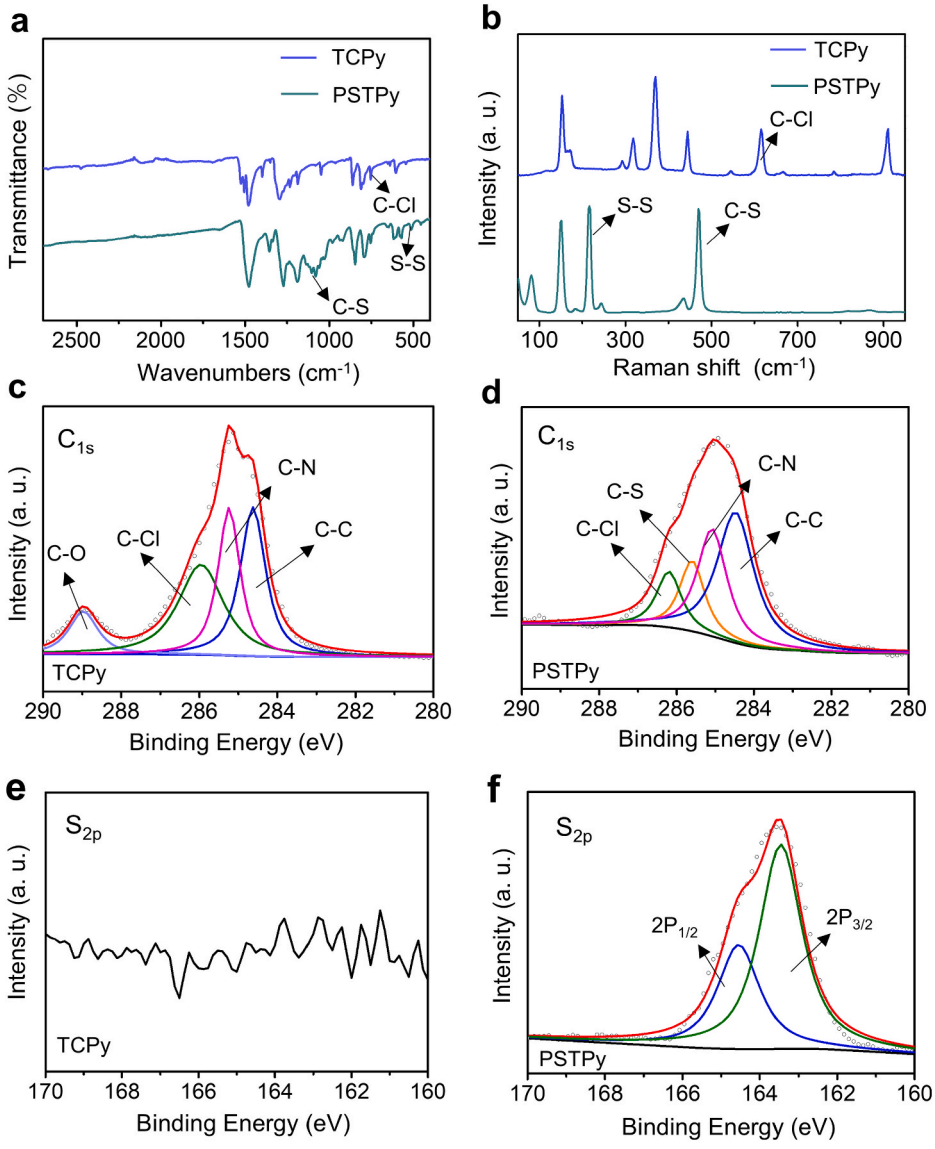

Fig. 2. (a) ATR-FTIR spectra of TCPy precursor and PSTPy gelatin. (b) Raman spectra of TCPy and PSTPy. (c, d) High-resolution XPS spectra at C 1 s level of (c) TCPy and (d) PSTPy. (e, f) High-resolution XPS spectra at S 2p level of (e) TCPy and (f) PSTPy.

underwent nucleophilic substitution reaction with S_6^{2-} ions, leading to the formation of an organosulfur polymer.[40] Raman spectroscopy analyses further support this structural transformation. In Fig. 2b, the Raman spectrum of crosslinked PSTPy gelatin exhibits two distinct peaks at 215 cm^{-1} and 490 cm^{-1}, corresponding to newly formed S—S—S bonds and C—S stretching mode within the polymer chain, respectively, confirming the crosslinking of organosulfur units.[37,40].

The high-resolution XPS spectra presented in Fig. 2c–d correspond to the C 1 s bands of TCPy and PSTPy, respectively. Different from the C 1 s XPS spectrum of TCPy precursor (Fig. 2c), the spectrum of PSTPy (Fig. 2d) shows four deconvoluted peaks at 284.6, 285.0, 285.5 and 286.2 eV, respectively, which could be attributed to C—C, C—N, C—S and C—Cl.[39] The decreased intensity of the C—Cl signal and the emergence of C—S signal confirm the substitution of Cl atoms and the formation of sulfur-containing polymer. Notably, the C 1 s XPS spectrum of the TCPy monomer shows a C—O signal, which is likely due to its hygroscopic nature and tendency to undergo partial oxidation when exposed to air, heat, or light during XPS sample preparation (Fig. 2c). In contrast, no C—O signal is observed in the C 1 s XPS spectrum of PSTPy (Fig. 2d), suggesting that its stable polymeric structure effectively resisted oxidation and moisture uptake. The S 2p spectrum of TCPy is free of S signal (Fig. 2e), while the S 2p spectrum of PSTPy showed two deconvoluted peaks at 163.2 eV and 164.9 eV, indicating successful reaction with polysulfides to form the organosulfur polymer. The distinct S 2p and N 1 s XPS signals observed in the S 2p and N 1 s spectra of PSTPy (Fig. 2f and Fig. S4) further substantiated the presence of both S and N atoms within the polymer, providing additional evidence of the nucleophilic substitution reaction and the resultant formation of a network-crosslinked polymer gelatin.

To assess the effect of TCPy additive on boosting the performance of Li-S batteries, electrochemical tests were conducted on the batteries assembled with and without TCPy additive (Fig. 3). Firstly, the concentration variation of TCPy additive on electrochemical performance were evaluated (Fig. 3a–b and Fig. S5). Among different concentrations (0, 30, 50, and 60 mM), the 50 mM concentration demonstrated the most favorable results, yielding enhanced charge-transfer kinetics and rate capability. Consequently, the assembly and testing of Li-S batteries in this study utilized a concentration of 50 mM TCPy additive in the electrolyte, unless otherwise noted.

By comparing the cyclic voltammetry (CV) curves during the initial five cycles at the same scan rate of 0.5 mV s^{-1} (Fig. 3c–d), it was evident that the Li-S batteries with TCPy additive exhibited improved CV repeatability, indicating enhanced reversibility. To investigate the specific impact of TCPy additive on the performance of Li-S batteries, comparative tests were conducted on the cycle performance and rate capability of Li-S batteries with and without TCPy additive. Fig. 3e illustrated the comparison of cycle performance at a current density of 2.0 C. When the battery was activated at a current density of 0.1 C, the discharge capacity of the battery with TCPy additive at the first cycle reached approximately 1650 mAh g^{-1}, with a coulomb efficiency of 100.0%. In contrast, the discharge capacity of the battery without TCPy additive at the first cycle was only 1490 mAh g^{-1}, with a coulomb efficiency of 87.6%. After 200 cycles at 2.0 C, the battery with TCPy additive maintained a specific capacity of 700.7 mAh g^{-1}, corresponding to a capacity retention rate of 87.3%, whereas the battery without TCPy additive exhibited a specific capacity of only 420.6 mAh g^{-1}, with a capacity retention rate of merely 50.3%. Furthermore, a comparison of the charge discharge curves in Fig. S6 revealed that, as the number of

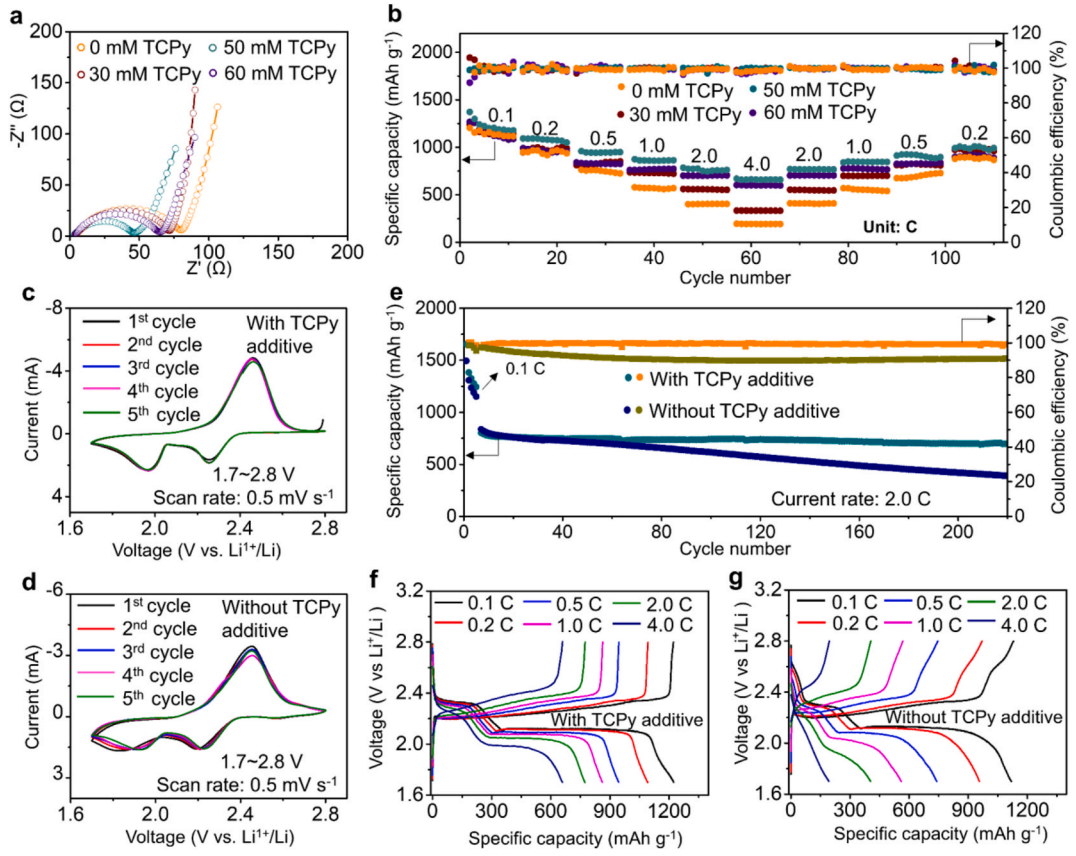

Fig. 3. (a) EIS spectra and (b) rate performances at various current rates between 0.1 C and 4.0 C of Li-S batteries with different concentrations (0, 30, 50, and 60 mM) of TCPy additive in the electrolyte. (c, d) CV curves during the initial 5 cycles of Li-S batteries (c) with and (d) without TCPy additive measured between 1.7–2.8 V *vs.* Li^+/Li at the scan rate of 0.5 mV s^{-1}. (e) Cycling performance and Coulombic efficiency of Li-S batteries with and without TCPy additive activated at 0.1 C and subsequently cycled at 2.0 C. (f, g) Discharge/charge profiles of Li-S batteries (f) with and (g) without TCPy additive tested at different current rates.

cycles increased, the voltage polarization of the Li-S battery without TCPy additive gradually increased, whereas the charge discharge voltage platform of the battery with TCPy additive showed minimal change after 200 cycles. Fig. S7 depicted the comparison of long cycle performance with and without TCPy additive at a current rate of 4.0 C. Clearly, the Li-S battery with TCPy additive exhibited higher initial capacity (603.6 mAh g^{-1}) and improved capacity retention (82.6%). Furthermore, Fig. S8 presented the cycling performance of Li-S battery with TCPy additive under an even higher current rate of 6.0 C. After 200 cycles, the battery still maintained a discharge capacity of 467.3 mAh g^{-1}, highlighting that the TCPy additive facilitated in-situ formation of PSTPy polymers, thus significantly enhancing the cycling stability of Li-S battery under high-rate charge–discharge conditions.

To further investigate the effect of TCPy additive, the rate capability of Li-S batteries was tested at various current densities, including 0.1 C, 0.2 C, 0.5 C, 1.0 C, 2.0 C, and 4.0 C (Fig. S9). Notably, when the current density increased to 4.0 C, the battery with TCPy additive maintained a specific capacity of 660 mAh g^{-1}, whereas the Li-S battery without TCPy additive only achieved 194 mAh g^{-1}. The corresponding discharge/charge profiles under different current densities were displayed in Fig. 3f–g. The Li-S battery with TCPy additive demonstrated higher capacity and lower voltage polarization, while the Li-S battery without TCPy additive exhibited higher polarization degree.

The practical potential of soft-packed Li||S batteries based on conventional sulfur/carbon nanotubes (S/CNTs) cathode and TCPy additive was studied by lighting a series of blue light-emitting diodes and performing long-term cycling tests (Fig. S10). The soft-packed Li||S/CNTs batteries with TCPy additive demonstrated promising electrochemical performance at both moderate and low current rates. At 0.5 C, a capacity of 964.9 mAh g^{-1} was delivered initially and 611.5 mAh g^{-1} remained after 98 cycles (Fig. S10c). At 0.1C, the battery maintained 1019.6 mAh g^{-1} after 20 cycles with an initial capacity of 1137.6 mAh g^{-1}, corresponding to 89.6% retention (Fig. S10d). These results highlight the good cycling stability and practical potential of TCPy-modified electrolytes for Li-S batteries.

Furthermore, the electrochemical performance of PSTPy gelatin, generated directly from the in-situ polymerization of TCPy and Li_2S_6, was tested as a cathode material (Fig. S11). The Li-S battery with PSTPy cathode demonstrated high capacity retention and good rate performance during cycling under high current rates. This further illustrated the viability of in-situ induced formation of PSTPy from TCPy and polysulfides for reversible energy storage. The formation of PSTPy gelatin significantly slowed down the dissolution of polysulfides, thereby enhancing the capacity retention at different current densities. Additionally, the nitrogen atom on the pyridine ring can adsorb polysulfide species and also improve the conductivity of the PSTPy gelatin, thereby further enhancing the rate performance.

The impact of TCPy additive on battery kinetics was further evalu-

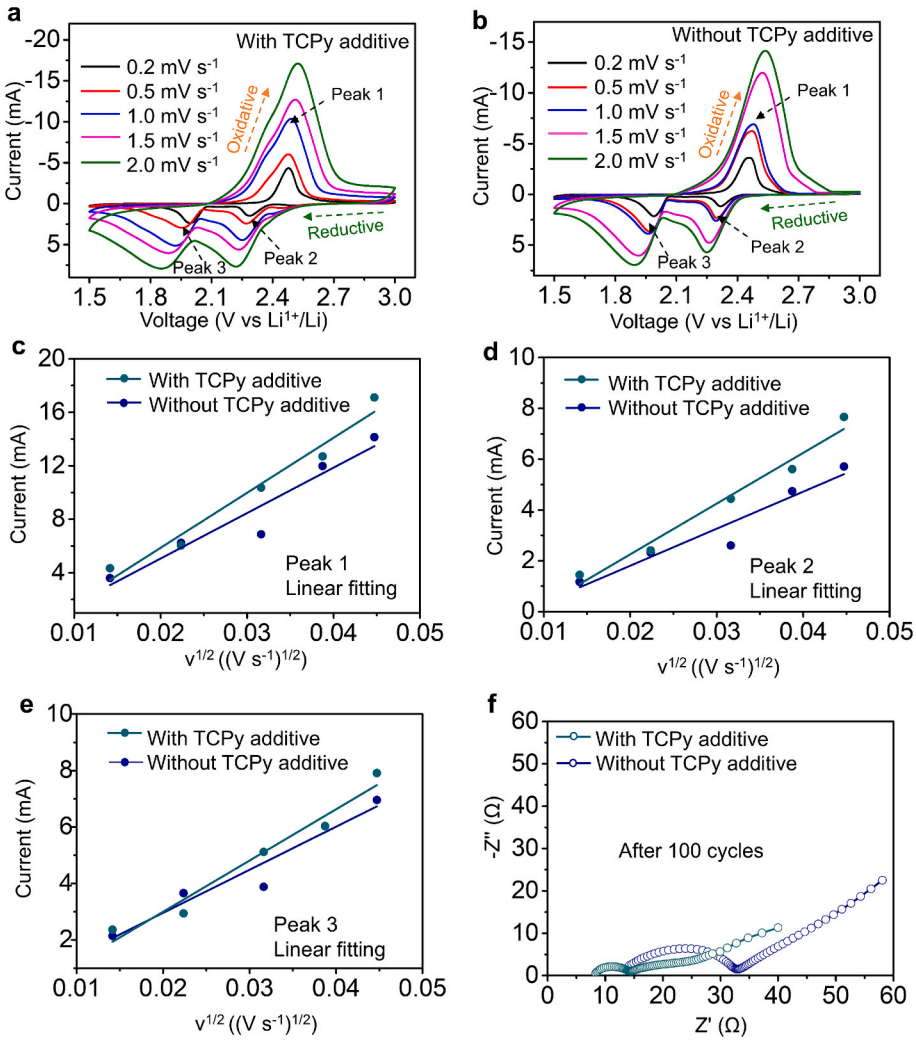

Fig. 4. (a, b) CV curves of S/CNTs cathodes in Li-S batteries (a) with and (b) without TCPy additive at different scan rates. (c-e) The corresponding CV peak current vs. the square root of scan rates ($v^{1/2}$) plots of S/CNTs cathodes in Li-S batteries with and without TCPy additive: (c) Peak 1, (d) Peak 2, and (e) Peak 3. (f) EIS spectra of S/CNTs cathodes in Li-S batteries with and without TCPy additive after 100 cycles.

ated by comparing the CV curves at different scan rates and impedance tests after extended battery cycling (Fig. 4). The CV curves obtained at different scan rates (Fig. 4a and b) demonstrated that the battery incorporating TCPy additive exhibited elevated response currents as the scan rate increased. For instance, at a scan rate of 2.0 mV s^{-1}, the oxidation peak current of the battery with TCPy additive reached approximately 17.5 mA, whereas the oxidation peak current of the battery without TCPy additive was below 15.0 mA. This observation suggests that the TCPy additive can greatly enhance the redox kinetics performance, potentially attributable to the conjugation of the pyrimidine ring and the electron-rich nature of the N atom. To provide a more intuitive representation of the specific effect of TCPy additive on the redox kinetics, a fitted straight line was obtained by correlating the peak current of the CV curve versus the square root of the scan rate at various scan rates (Fig. 4c–e). The diffusion coefficient of lithium-ion (Li^+) in the battery can be calculated according to the Randles-Sevcik formula[41]:

$$I_p = 2.65 \times 10^5 n^{1.5} S D_{Li^+}{}^{0.5} C v^{0.5} \quad (1)$$

where *Ip* is the peak current (A mg^{-1}), n is the charge transfer number, *S* is the area of the electrode (cm^2), D_{Li+} is the diffusion coefficient of Li^+ (cm^2 s^{-1}), *C* is the amount of Li^+ in the electrolyte concentration (mol cm^{-3}), and ν is the scan rate (V s^{-1}). Since the influencing factors of the slope of the fitting line are all constants except for D_{Li+}, the slope is only related to the diffusion coefficient of Li^+. By comparing the slopes of the straight fitted lines for the three peaks in Fig. 4c–e, the battery with the TCPy additive exhibits a larger slope, with the specific values listed in Table S1. This indicates a higher Li^+ diffusion coefficient, further confirming the enhancement of redox kinetics by TCPy additive. This reflects the help of nitrogen atoms in the pyrimidine structure to improve electrical conductivity.

Furthermore, electrochemical impedance spectroscopy (EIS) tests were conducted to assess the impact of TCPy additive on the conductivity. Electrochemical impedance tests were carried out on the batteries after galvanostatic cycling (Fig. 4f). The EIS results after 100 consecutive charge–discharge cycles revealed a reduction in charge transfer impedance to varying degrees. Specifically, the battery with TCPy additive showcased a charge transfer impedance of approximately 6.0 Ω, while the battery without TCPy additive exhibited a charge transfer impedance of about 19.0 Ω. The comparison of the impedance after cycling indicates that the sulfur-containing PSTPy gelatin generated by the inclusion of TCPy additive can enhance the conductivity and charge transfer capability of the Li-S batteries.

To investigate the interactions between TCPy and polysulfides, a symmetrical battery was assembled utilizing TCPy-loaded carbon paper electrodes and 0.40 M Li_2S_6 in DME/DOL electrolyte (1:1 in volume). Aa a control, another symmetrical battery was assembled using carbon black (CB) electrodes. To assess the electrochemical behavior of both symmetrical batteries, CV analyses were performed within a voltage range of −1.0 V to 1.0 V at a scanning rate of 1.0 mV s^{-1} (Fig. 5a). The peak intensity of TCPy based symmetrical battery was significantly higher than that of CB based symmetrical battery, suggesting the formation of chemical bonds between TCPy and polysulfides during battery cycling. Furthermore, the CV curve of TCPy based symmetrical battery exhibits a narrower voltage range at the position of the redox peak compared to that of CB based symmetrical battery, accompanied by a sharper peak shape. This observation indicates that TCPy not only effectively bind with polysulfides, but also mitigate polarization effects and promote the polysulfide conversion kinetics.

To further explore the role of TCPy additive on alleviating the shuttle effect, a series of characterizations on the S/CNTs cathodes with and without TCPy additive were conducted. Specifically, the Li-S batteries with and without TCPy additive were firstly discharged to 2.20 V after 200 cycles. Then, the batteries were disassembled in an Ar-filled glovebox, and the S/CNTs cathodes were immersed in DME solution to

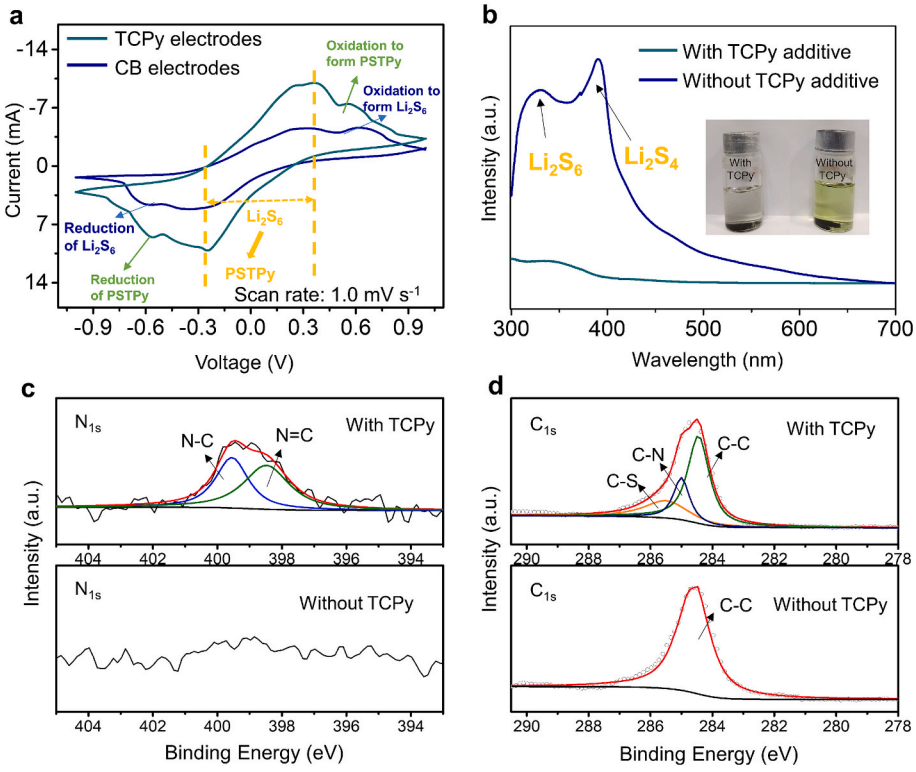

Fig. 5. (a) CV curves of symmetric batteries based on TCPy or carbon black (CB) electrodes from −1.0 V to 1.0 V at a scan rate of 1.0 mV s^{-1}. (b) UV–Vis absorption spectra and corresponding photographs of the DME solutions soaked with S/CNTs cathodes retrieved from Li-S batteries with or without TCPy additive after 200 cycles. (c, d) ex-situ (c) N 1 s and (d) C 1 s XPS spectra of the S/CNTs cathodes retrieved from the Li-S batteries with or without TCPy additive discharged to 2.20 V after 200 cycles.

dissolve the polysulfides. The solutions were analyzed using ultraviolet–visible (UV–Vis) absorption spectroscopy within the range of 300–700 nm (Fig. 5b). For the sample without TCPy additive, an evident absorption peak between 300–400 nm was observed, indicating the generation of polysulfides[42]. In contrast, for the sample with TCPy additive, almost no absorption peak in the aforementioned range was exhibited, indicating the significant reduction of polysulfide dissolution by TCPy additive. Furthermore, the visual comparison in the inset of Fig. 5b clearly indicated that the color of DME solution soaked by S/CNTs cathode with TCPy additive appeared significantly lighter, almost transparent and colorless, whereas the DME solution soaked by S/CNTs cathode without TCPy additive exhibited a strong yellow color. This observation directly demonstrates the inhibitory effect of TCPy additive on polysulfide dissolution. Scanning electron microscopy (SEM) and corresponding elemental mapping images were obtained for the two cleaned electrodes in Fig. 5b, and the results were presented in Fig. S12. In the presence of TCPy additive, the morphology of S/CNTs cathode after cycling appeared more regular, and the distribution of sulfur (S) elements was denser, indicating the inhibition of the shuttle effect by TCPy additive. The uniform distribution of N elements represented the formation of PSTPy gelatin polymer. Additionally, ex-situ XPS analyses were conducted on the S/CNTs cathode samples with and without TCPy additive discharged to 2.20 V to verify the cathode structure and the formation of sulfur-containing polymer (Fig. 5c–d and Fig. S13). For the sample with TCPy additive, the presence of characteristic N 1 s signals confirm the successful incorporation of TCPy with polysulfides that results in the formation of insoluble PSTPy gelatin polymer (Fig. 5c). Furthermore, the appearance of C–S signal in the C 1 s spectrum with a binding energy around 285.5 eV provided further evidence of the successful polymerization and the bonding structure of PSTPy (Fig. 5d). [43] In addition, ex-situ Raman spectra of S/CNTs cathodes discharged to 2.20 V further support this conclusion (Fig. S14). The S/CNTs cathode discharged to 2.20 V with TCPy additive exhibits a distinct C—S vibration peak at 490 cm^{-1}, which is absent in the pristine state, indicating the formation of PSTPy (Fig. S14a). In contrast, the Raman spectrum of S/CNTs cathode discharged to 2.20 V without TCPy is nearly identical to that of the pristine S/CNTs cathode, with no detectable C—S bond signals, indicating significant polysulfide dissolution (Fig. S14b).

The enhancement effect of TCPy additive on the electrolyte performance was investigated through a series of control experiments (Fig. S15–S16), including the Tafel curve measurements on Li-Li symmetrical batteries, the linear sweep voltammetry measurements on Li|| stainless-steel half batteries, and the voltage–time measurements during Li deposition/stripping on Li-Li symmetrical batteries. It was found that the exchange current density and voltage window of ether-based electrolyte were enhanced by the inclusion of TCPy additive (Fig. S15). Furthermore, the Li^+ diffusion kinetics were effectively promoted, thereby facilitating the rapid transfer and conversion of Li ions. These results confirmed that the electrochemical performance and stability of ether-based electrolyte were positively influenced by the TCPy additive, leading to enhanced performance of Li-S batteries.

On the other hand, the influence of TCPy additive on lithium metal electrode was investigated through SEM and elemental mapping characterizations of recycled lithium anodes (Fig. S17–S19). The surface morphology of lithium anodes after cycling was displayed in Fig. S17. A smooth and flat surface was observed on the lithium anode retrieved from the battery with TCPy additive after 200 cycles (Fig. S17a–S17b), while an uneven surface with numerous wrinkles was observed on the lithium anode retrieved from the battery without TCPy additive (Fig. S17c–S17d). Furthermore, the battery with TCPy additive demonstrated a reduced presence of S species on the surface of lithium anode after cycling, with a sparser distribution (Fig. S18a–S18c and Fig. S19a). In contrast, the discharging process of Li-S batteries without TCPy additive was greatly affected by the shuttle effect, which resulted in a higher degree of polysulfide dissolution and the irreversible deposition of Li_2S on the surface of lithium anode after cycling (Fig. S18d-S18f and Fig. S19b).

3. Conclusion

In summary, we introduced TCPy as a novel electrolyte additive for Li-S batteries, aimed at mitigating the shuttle effect through the in-situ formation of insoluble 3D-crosslinked organosulfur polymer PSTPy. During the discharge process, the chlorine atoms in TCPy initiated nucleophilic substitution reactions with polysulfides, resulting in the formation of PSPTy gelatin that effectively suppressed the dissolution and diffusion of polysulfides. Additionally, the nitrogen atoms in TCPy exhibited strong chemical adsorption properties towards polysulfides, further inhibiting their dissolution. Incorporating the TCPy-modified electrolyte into Li-S batteries significantly enhanced cycle stability and rate performance, with a specific capacity of 660 mAh g^{-1} retained even at a high current density of 4.0 C. Furthermore, the Li^+ deposition/stripping kinetics and cycling stability of lithium anode were also enhanced. Notably, the PSPTy gelatin are generated by the in-situ crosslinking reaction of organic small-molecule TCPy additive with polysulfides, offering advantages such as easy access to raw materials and simplicity of operation. This approach stands as a highly effective and promising strategy for suppressing the shuttle effect, underscoring the substantial potential of functional electrolyte additives to elevate the performance of rechargeable alkali metal–chalcogen batteries.

Author contributions

Z. J. and X. M. conceived the idea of this study. X. M. performed the preparation of the samples. X. M. and X. S. performed the FT-IR, Raman and XPS analyses. X. M., Y. W. and T. S. performed the electrochemical measurements. X. M., J. L., Z. W., L. Q., H. L., T. Y., H. W., and Z. T. contributed to the data analysis. X. M., Y. Y., L. S., and Z. J. analyzed the data and wrote the paper. Z. J. revised the manuscript and supervised the project. All authors discussed the results and commented on the manuscript.

CRediT authorship contribution statement

Xingkai Ma: Writing – original draft, Data curation, Conceptualization. **Xinmei Song:** Methodology. **Yaoda Wang:** Validation. **Junchuan Liang:** Methodology. **Tianyu Shen:** Visualization. **Zuoao Wu:** Investigation. **Lina Qin:** Software. **Huan Li:** Visualization. **Tianchen Yu:** Software. **Huaizhu Wang:** Methodology. **Zuoxiu Tie:** Formal analysis. **Yichao Yan:** Validation. **Lin Sun:** Formal analysis. **Zhong Jin:** Writing – review & editing, Writing – original draft.

Declaration of competing interest

The authors declare that they have no known competing financial interests or personal relationships that could have appeared to influence the work reported in this paper.

Acknowledgements

The authors appreciate the financial support from the National Natural Science Foundation of China (22479074 and 22475096), the General Project of the Joint Fund of Equipment Pre-research and the Ministry of Education (8091B02052407), the Natural Science Foundation of Jiangsu Province (BK20240400 and BK20241236), the Science and Technology Major Project of Jiangsu Province (BG2024013), the Scientific and Technological Achievements Transformation Special Fund of Jiangsu Province (BA2023037), the Academic Degree and Postgraduate Education Reform Project of Jiangsu Province (JGKT24_C001), the Key Core Technology Open Competition Project of Suzhou City (SYG2024122), the open research fund of Suzhou Laboratory (SZLAB-1308-2024-TS005), the Gusu Leading Talent Program of

Scientific and Technological Innovation and Entrepreneurship of Wujiang District in Suzhou City (ZXL2021273), and the Chenzhou National Sustainable Development Agenda Innovation Demonstration Zone Provincial Special Project (2023sfq11).

Appendix A. Supplementary data

Supplementary data to this article can be found online at https://doi.org/10.1016/j.cej.2025.162921.

Data availability

Data will be made available on request.

References

[1] Y. Liu, S. Liu, G.R. Li, X.P. Gao, Strategy of Enhancing the Volumetric Energy Density for Lithium-Sulfur Batteries, Adv. Mater. 33 (8) (2021) 2003955, https://doi.org/10.1002/adma.202003955.

[2] L. Wang, X. Yin, C. Jin, C. Lai, G. Qu, G. Zheng, Cathode-Supported-Electrolyte Configuration for High-Performance All-Solid-State Lithium-Sulfur Batteries, ACS Appl. Mater. Interfaces 3 (12) (2020) 11540–11547, https://doi.org/10.1021/acsaem.0c02347.

[3] C. Zhao, G. Xu, Z. Yu, L. Zhang, I. Hwang, Y. Mo, Y. Ren, L. Cheng, C. Sun, Y. Ren, X. Zuo, J. Li, S. Sun, K. Amine, T. Zhao, A high-energy and long-cycling lithium-sulfur pouch cell via a macroporous catalytic cathode with double-end binding sites, Nat. Nanotechnol. 16 (2021) 224, https://doi.org/10.1038/s41565-020-00797-w.

[4] Z. Liang, D. Yang, P. Tang, C. Zhang, J. Biendicho, Y. Zhang, J. Llorca, X. Wang, J. Li, M. Heggen, J. David, R.E. Dunin-Borkowski, Y. Zhou, J.R. Morante, A. Cabot, J. Arbiol, Atomically dispersed Fe in a C_2N Based Catalyst as a Sulfur Host for Efficient Lithium-Sulfur Batteries, Adv. Energy Mater. 11 (5) (2021) 2003507, https://doi.org/10.1002/aenm.202003507.

[5] Z. Wang, Y. Dong, H. Li, Z. Zhao, H. Wu, C. Hao, S. Liu, J. Qiu, X. Lou, Enhancing lithium-sulphur battery performance by strongly binding the discharge products on amino-functionalized reduced graphene oxide, Nat. Commun. 5 (2014) 5002, https://doi.org/10.1038/ncomms6002.

[6] Y. Ren, B. Wang, H. Liu, H. Wu, H. Bian, Y. Ma, H. Lu, S. Tang, X. Meng, CoP nanocages intercalated MXene nanosheets as a bifunctional mediator for suppressing polysulfide shuttling and dendritic growth in lithium-sulfur batteries, Chem. Eng. J. 450 (3) (2022) 138046, https://doi.org/10.1016/j.cej.2022.138046.

[7] Y. Xiao, Y. Xiang, S. Guo, J. Wang, Y. Ouyang, D. Li, Q. Zeng, W. Gong, L. Gan, Q. Zhang, S. Huang, An ultralight electroconductive metal-organic framework membrane for multistep catalytic conversion and molecular sieving in lithium-sulfur batteries, Energy Storage Mater. 51 (2022) 882–889, https://doi.org/10.1016/j.ensm.2022.07.018.

[8] B. Jin, L. Yang, J. Zhang, Y. Cai, J. Zhu, J. Lu, Y. Hou, Q. He, H. Xing, X. Zhan, F. Chen, Q. Zhang, Bioinspired Binders Actively Controlling Ion Migration and Accommodating Volume Change in High Sulfur Loading Lithium-Sulfur Batteries, Adv. Energy Mater. 9 (48) (2019) 1902938, https://doi.org/10.1002/aenm.201902938.

[9] L. Ma, G. Zhu, W. Zhang, P. Zhao, Y. Hu, Y. Wang, R. Chen, T. Chen, Z. Tie, J. Liu, Z. Jin, Three-dimensional spongy framework as superlyophilic, strongly absorbing, and electrocatalytic polysulfide reservoir layer for high-rate and long-cycling lithium-sulfur batteries, Nano Res. 11 (2018) 6436–6446, https://doi.org/10.1007/s12274-018-2168-8.

[10] N. Xu, T. Qian, X.J. Liu, J. Liu, Y. Chen, C.L. Yang, Greatly Suppressed Shuttle Effect for Improved Lithium Sulfur Battery Performance through Short Chain Intermediates, Nano Lett. 17 (1) (2017) 538–543, https://doi.org/10.1021/acs.nanolett.6b04610.

[11] H.H. Chen, Y.W. Xiao, C. Chen, J.Y. Yang, C. Gao, Y.S. Chen, J.S. Wu, Y. Shen, W. N. Zhang, S. Li, F.W. Huo, B. Zheng, Conductive MOF-Modified Separator for Mitigating the Shuttle Effect of Lithium-Sulfur Battery through a Filtration Method, ACS Appl. Mater. Interfaces 11 (12) (2019) 11459–11465, https://doi.org/10.1021/acsami.8b22564.

[12] C. Su, M. He, R. Amine, Z. Chen, K. Amine, The Relationship between the Relative Solvating Power of Electrolytes and Shuttling Effect of Lithium Polysulfides in Lithium-Sulfur Batteries, Angew. Chem. Int. Ed. 57 (37) (2018) 12033–12036, https://doi.org/10.1002/anie.201807367.

[13] Y. He, Y. Qiao, Z. Chang, X. Cao, M. Jia, P. He, H. Zhou, Developing A "Polysulfide-Phobic" Strategy to Restrain Shuttle Effect in Lithium-Sulfur Batteries, Angew. Chem. Int. Ed. 58 (34) (2019) 11774–11778, https://doi.org/10.1002/anie.201906055.

[14] L. Li, Y. Shan, The Use of Graphene and Its Composites to Suppress the Shuttle Effect in Lithium-Sulfur Batteries, New Carbon Mater. 36 (2) (2021) 336–349, https://doi.org/10.1016/s1872-5805(21)60023-9.

[15] L. Guo, X. Zhang, M. Xiao, S. Wang, D.M. Han, Y.Z. Meng, Two-Dimensional Materials Modified Separator Strategies of Suppressing the Shuttle Effect in Lithium-Sulfur Batteries, Prog. Chem. 33 (2021) 1198–1206, https://doi.org/10.7536/PC200721.

[16] T. Zhou, Z. Shen, Y. Wu, T. Han, M. Zhu, X. Qiao, Y. Zhu, H. Zhang, J. Liu, A yolk-shell Fe_3O_4@void@carbon nanochain as shuttle effect suppressive and volume-change accommodating sulfur host for long-life lithium-sulfur batteries, Nanoscale 13 (16) (2021) 7744–7750, https://doi.org/10.1039/d1nr00658d.

[17] C. Long, L. Li, M. Zhai, Y. Shan, Facile preparation and electrochemistry performance of quasi solid-state polymer lithium-sulfur battery with high-safety and weak shuttle effect, J. Phys. Chem. Solid 134 (2019) 255–261, https://doi.org/10.1016/j.jpcs.2019.06.017.

[18] Q. Jin, L. Li, H. Wang, H. Gao, C. Zhu, X.T. Zhang, Dual effects of the carbon fibers/$Ti_3C_2T_x$ interlayer on retarding shuttle of polysulfides for stable Lithium-Sulfur batteries, Electrochim. Acta 312 (2019) 149–156, https://doi.org/10.1016/j.electacta.2019.04.182.

[19] Y. Wang, Y. Pu, L. Ya, Y. Zhang, C. Liu, Q. Wang, H. Wu, Synergistic Effect of WN/Mo_2C Embedded in Bioderived Carbon Nanofibers: A Rational Design of a Shuttle Inhibitor and an Electrocatalyst for Lithium-Sulfur Batteries, ACS Appl. Mater. Interfaces 14 (16) (2022) 18578–18588, https://doi.org/10.1021/acsami.2c02836.

[20] K. Sun, C. Wang, Y. Dong, P. Guo, P. Cheng, Y. Fu, D. Liu, D. He, S. Das, Y. Negishi, Ion-Selective Covalent Organic Framework Membranes as a Catalytic Polysulfide Trap to Arrest the Redox Shuttle Effect in Lithium-Sulfur Batteries, ACS Appl. Mater. Interfaces 14 (3) (2022) 4079–4090, https://doi.org/10.1021/acsami.1c20398.

[21] D. Zhang, W. Huang, Z. Li, Y. Li, C. Xiang, M. Chen, X. Wang, X. Wang, Core-Shell Structure S@PPy/CB with High Electroconductibility to Effective Confinement Polysulfide Shuttle Effect for Advanced Lithium-Sulfur Batteries, Energy Fuel 35 (12) (2021) 10181–10189, https://doi.org/10.1021/acs.energyfuels.1c00300.

[22] S. Chung, A. Manthiram, Current status and future prospects of metal-sulfur batteries, Adv. Mater. 31 (27) (2019) 1901125, https://doi.org/10.1002/adma.201901125.

[23] S. Ruan, Z. Huang, W. Cai, C. Ma, X. Liu, J. Wang, W. Qiao, L. Ling, Enabling rapid polysulfide conversion kinetics by using functionalized carbon nanosheets as metal-free electrocatalysts in durable lithium-sulfur batteries, Chem. Eng. J. 385 (2020) 123840, https://doi.org/10.1016/j.cej.2019.123840.

[24] F. Li, J. Tao, Z. Zou, C. Li, Z. Hou, J. Zhao, Aminomethyl-Functionalized Carbon Nanotubes as a Host of Small Sulfur Clusters for High-Performance Lithium-Sulfur Batteries, ChemSusChem 13 (2020) 2761–2768, https://doi.org/10.1002/cssc.202000289.

[25] H.M. Kim, J.Y. Hwang, S. Bang, H. Kim, M.H. Alfaruqi, J. Kim, C.S. Yoon, Y.K. Sun, Tungsten Oxide/Zirconia as a Functional Polysulfide Mediator for High-Performance Lithium-Sulfur Batteries, ACS Energy Lett. 5 (10) (2020) 3168–3175, https://doi.org/10.1021/acsenergylett.0c01511.

[26] L. Wang, Y.H. Song, B.H. Zhang, Y.T. Liu, Z.Y. Wang, G.R. Li, S. Liu, X.P. Gao, Spherical Metal Oxides with High Tap Density as Sulfur Host to Enhance Cathode Volumetric Capacity for Lithium-Sulfur Battery, ACS Appl. Mater. Interfaces 12 (5) (2020) 5909–5919, https://doi.org/10.1021/acsami.9b20111.

[27] Z.Z. Cheng, Y.X. Wang, W.J. Zhang, M. Xu, Boosting Polysulfide Conversion in Lithium-Sulfur Batteries by Cobalt-Doped Vanadium Nitride Microflowers, ACS Appl. Mater. Interfaces 3 (5) (2020) 4523–4530, https://doi.org/10.1021/acsaem.0c00205.

[28] T.T. Li, C. He, W.X. Zhang, Two-dimensional porous transition metal organic framework materials with strongly anchoring ability as lithium-sulfur cathode, Energy Storage Mater. 25 (2020) 866–875, https://doi.org/10.1016/j.ensm.2019.09.003.

[29] G.J. Gao, W.J. Feng, W.X. Su, S.J. Wang, L.J. Chen, M.M. Li, C.K. Song, Preparation and Modification of MIL-101(Cr) Metal Organic Framework and Its Application in Lithium-Sulfur Batteries, Int. J. Electrochem. Sci. 15 (2) (2020) 1426–1436, https://doi.org/10.20964/2020.02.26.

[30] F.L. Zhu, Y.L. Tao, H.F. Bao, X.S. Wu, C. Qin, X.L. Wang, Z.M. Su, Ferroelectric Metal-Organic Framework as a Host Material for Sulfur to Alleviate the Shuttle Effect of Lithium-Sulfur Battery, Chem. A Eur. J. 26 (61) (2020) 13779–13782, https://doi.org/10.1002/chem.202002198.

[31] W.J. Chung, J.J. Griebel, E.T. Kim, H. Yoon, A.G. Simmonds, H.J. Ji, P.T. Dirlam, R. S. Glass, J.J. Wie, N.A. Nguyen, B.W. Guralnick, J. Park, A. Somogyi, P. Theato, M. E. Mackay, Y.-E. Sung, K. Char, J. Pyun, The use of elemental sulfur as an alternative feedstock for polymeric materials, Nature Chemistry 5 (2013) 518–524, https://doi.org/10.1038/nchem.1624.

[32] J. Park, E.T. Kim, C. Kim, J. Pyun, H.-S. Jang, J. Shin, J.W. Choi, K. Char, Y.-E. Sung, The importance of confined sulfur nanodomains and adjoining electron conductive pathways in subreaction regimes of Li-S batteries, Adv. Energy Mater. 7 (2017) 1700074, https://doi.org/10.1002/aenm.201700074.

[33] S.H. Je, T.H. Hwang, S.N. Talapaneni, O. Buyukcakir, H.J. Kim, J.-S. Yu, S.-G. Woo, M.C. Jang, B.K. Son, A. Coskun, J.W. Choi, Rational sulfur cathode design for lithium–sulfur batteries: sulfur-embedded benzoxazine polymers, ACS Energy Lett. 1 (3) (2016) 566–572, https://doi.org/10.1021/acsenergylett.6b00245.

[34] S. Zeng, L. Li, L. Xie, D. Zhao, N. Wang, S. Chen, Conducting Polymers Crosslinked with Sulfur as Cathode Materials for High-Rate, Ultralong-Life Lithium-Sulfur Batteries, ChemSusChem 10 (2017) 3378–3386, https://doi.org/10.1002/cssc.201700913.

[35] X. Chen, L. Peng, L. Wang, J. Yang, Z. Hao, J. Xiang, K. Yuan, Y. Huang, B. Shan, L. Yuan, J. Xie, Ether-compatible sulfurized polyacrylonitrile cathode with excellent performance enabled by fast kinetics via selenium doping, Nat. Commun. 10 (2019) 1021, https://doi.org/10.1038/s41467-019-08818-6.

[36] W. Yan, K. Yan, G. Kuang, Z. Jin, Fluorinated quinone derived organosulfur copolymer cathodes for long-cycling, thermostable and flexible lithium–sulfur batteries, Chem. Eng. J. 424 (2021) 130316, https://doi.org/10.1016/j.cej.2021.130316.

[37] A. Tao, K. Zhang, X. Ma, X. Song, J. Liang, Y. Wang, Y. Liu, L. Jin, Z. Tie, Z. Jin, Building lithium-polycarbonsulfide batteries with high energy density and long cycling life, ACS Energy Lett. 8 (2023) 79–89, https://doi.org/10.1021/acsenergylett.2c02107.
[38] M.V. Stasevych, M.Y. Plotnikov, M.O. Platonov, S.I. Sabat, R.Y. Musyanovych, V. P. Novikov, Sulfur-containing derivatives of 1,4-naphthoquinone, part 1: Disulfide synthesis, Heteroat. Chem 16 (3) (2005) 205–211, https://doi.org/10.1002/hc.20112.
[39] J. Xu, F. Yu, J. Hua, W. Tang, C. Yang, S. Hu, S. Zhao, X. Zhang, Z. Xin, D. Niu, Donor dominated triazine-based microporous polymer as a polysulfide immobilizer and catalyst for high-performance lithium-sulfur batteries, Chem. Eng. J. 392 (2020) 123694, https://doi.org/10.1016/j.cej.2019.123694.
[40] X. Zhang, G. Hu, K. Chen, L. Shen, R. Xiao, P. Tang, C. Yan, H.-M. Cheng, Z. Sun, F. Li, Structure-related electrochemical behavior of sulfur-rich polymer cathode with solid-solid conversion in lithium-sulfur batteries, Energy Storage Mater. 45 (2022) 1144–1152, https://doi.org/10.1016/j.ensm.2021.11.014.
[41] R. Sun, Y. Bai, M. Luo, Z. Wang, W. Sun, K. Sun, Enhancing Polysulfide Confinement and Electrochemical Kinetics by Amorphous Cobalt Phosphide for Highly Efficient Lithium-Sulfur Batteries, ACS Nano 15 (1) (2021) 739–750, https://doi.org/10.1021/acsnano.0c07038.
[42] H. Xu, Y. Shi, S. Yang, B. Li, A linear molecule sulfur-rich organic cathode material for high performance lithium–sulfur batteries, J. Power Sources 430 (2019) 210–217, https://doi.org/10.1016/j.jpowsour.2019.05.022.
[43] Z. Yang, F. Wang, Z. Hu, J. Chu, H. Zhan, X. Ai, Z. Song, Room-Temperature All-Solid-State Lithium–Organic Batteries Based on Sulfide Electrolytes and Organodisulfide Cathodes, Adv. Energy Mater. 11 (2021) 2102962, https://doi.org/10.1002/aenm.202102962.